University of Delaware
Newark, De 19716-3820
Ph: 302/831-6200
Fax: 302/831-6226
www.udel.edu/iec

INSTITUTE OF ENERGY CONVERSION

UNITED STATES DEPARTMENT OF ENERGY
UNIVERSITY CENTER OF EXCELLENCE
FOR PHOTOVOLTAIC RESEARCH AND EDUCATION

October 23, 2007

Bolko von Roedern
National Renewable Energy Laboratory
1617 Cole Boulevard
Golden, CO 80401

Re: NREL Subcontract #ADJ-1-30630-12
D.5.21

Dear Bolko,

This report covers research conducted at the Institute of Energy Conversion (IEC) for the period of July 1, 2007 to July 31, 2007, under the subject subcontract. The report highlights progress and results obtained under Task 2 (CIS-based solar cells).

Task 2: $CuInSe_2$-based Solar Cells

In-Line Evaporation of $Cu(InGa)Se_2$

Reactor Source Control and Modeling

The PhD thesis dealing with control and modeling of the sources that was supported by this program has been completed. Below is the Abstract of the thesis by Dr. K. Mukati:

AN ALTERNATIVE STRUCTURE FOR NEXT GENERATION REGULATORY CONTROLLERS AND SCALE-UP OF CU(INGA)SE2 THIN FILM CO-EVAPORATIVE PHYSICAL VAPOR DEPOSITION PROCESS

by

Kapil Mukati

A Dissertation submitted to the Faculty of the University of Delaware in partial fulfillment of the requirements for the degree of Doctor of Philosophy in Chemical Engineering

Abstract

Process control systems have three key performance attributes: Set-point tracking (T) – ability to cause the process output to follow set-point changes rapidly and faithfully; Disturbance rejection (D) --- ability to counteract the effects of external disturbances; and Robustness ® --- ability to remain stable and perform well in the face of inevitable plant/model mismatch. A controller whose tuning constants are related directly to these performance attributes will have definite advantages over other controllers. However, the popular PID controller, even though simple, has an intrinsic structure that results in a complicated, hence non-transparent, relationship between its tuning parameters and the three controller performance attributes, limiting the controller's achievable performance and making tuning arguably more complex than necessary. In order to overcome the weaknesses of the PID controller, we have developed an alternative regulatory controller (the RTDA controller) having the following salient features: it requires precisely the same information that is required for tuning PID controllers; its tuning parameters are directly related to the three key controller attributes of R, T and D (an auxiliary fourth parameter, influences the overall controller aggressiveness (A)); all four tuning parameters are normalized to lie between 0 and 1; and the magnitude of a tuning parameter is related to performance aggressiveness, where the higher magnitudes signify conservative performance in the attribute of interest. In addition, the proposed predictive controller is not any more complicated to implement, in either software or hardware, than the PID controller.

In order to study how the choices of various RTDA controller parameter values jointly and individually affect closed-loop stability, theoretical robust stability analysis is performed. The results of this analysis are subsequently used to develop systematic strategies for choosing the RTDA controller parameters that provide the best possible trade-off between robust stability and performance. The design and implementation of the RTDA controller in practice is illustrated experimentally using two processes: a lab-scale four-tank process with time delay and a pilot-scale physical vapor deposition process with nonlinear dynamics. These experiments demonstrate the RTDA controller's improved performance over PID controllers. The RTDA control scheme is also extended to integrating and open-loop unstable processes.

A pilot-scale co-evaporative physical vapor deposition (PVD) process for manufacture of copper indium gallium diselenide ($Cu(InGa)Se_2$) thin films is chosen to validate the proposed RTDA controller experimentally, since robust control of film thickness and composition set-points for long deposition times cannot be achieved without effective base regulatory control. However, unlike film thickness and composition set-points that can be achieved with proper process control design, achieving film thickness uniformity across large area substrates is a process design issue. To achieve good process performance, the process design issues are addressed first, and then the regulatory controller design is improved.

The work presented in Part II of this thesis is focused mainly on the evaporation source design. Such a study requires not only the detailed knowledge of the evaporation source

temperature profile, but also accurate estimation of nozzle flow properties (effusion rates and vapor flux distribution). A three-dimensional first-principles electro-thermal model of the source is developed using COMSOL Multiphysics software, and Direct Simulation Monte Carlo (DSMC) technique is employed to predict accurately the nozzle flow properties for any given nozzle geometry and evaporant. These models are validated experimentally, and subsequently used to design evaporation sources that not only achieve the targeted film thickness uniformity, but also maximize the material utilization efficiency.

System Maintenance and Upgrade

Early during the present reporting period, the in-line system showed a major leak. The leak was traced to the ferrofluidic rotary feed through driving the pick-up roll. Delivery time of a new feedthrough was quoted to be 4 to 6 weeks and an order was placed for two new feedthroughs. Because of such a long down time it was decided to perform a long overdue overhaul of the system.

The following system upgrades were performed:

- Fabrication and installation and testing of a new substrate heating assembly.
- Putting in service a back-up computer system to operate the reactor in case the main computer malfunctions.
- An upgrade of the In source to the design being used in the Cu and Ga sources.
- Replacement of all the control thermocouples in the sources. The new thermocouples are HfO_2 insulated rather than BeO since the latter type is not being manufactured anymore due to the health considerations. Because of the new type of insulator the temperature offset on the thermocouples has to be determined again.
- Diffusion and mechanical pumps were serviced.

When the feedthroughs were received it was decided to have them water cooled to increase operational lifetime. They are installed on the reactor with water cooling lines. Leak checking of the system found other leaks that were repaired. The system is now fully operational and will go through testing and calibration before experiments to determine the limit of $Cu(InGa)Se_2$ deposition time and the effects of higher speed deposition will resume.

Increased V_{OC} for Improved Module Performance

Composition Control for $Cu(InGa)(SeS)_2$ Evaporation

Efforts on wide bandgap $Cu(InGa)(SeS)_2$ alloys for increased V_{OC} continue to focus on controlling the composition of evaporated films to enable the effects of different compositions and through-film compositional profiles on devices to be characterized. We have previously determined the effect of changes in [Cu]/[In+Ga] and [Ga]/[In+Ga] on the relative S incorporation at substrate temperature (T_{SS}) = 550°C. In this work, the dependence of the relative Se and S incorporation chalcogen in $Cu(InGa)(SeS)_2$ on the substrate temperature was characterized with various [S]/[Se+S] flux rate ratios of at T_{SS} = 300°C, 450°C, and 550°C. All films were grown with excess chalcogen species in the flux with [S+Se]/[Cu+In+Ga]~10, and both flux rate ratios of [S]/[Cu+In+Ga] and [Se]/[Cu+In+Ga] were greater than unity throughout all experiments. The Ga content was adjusted to be [Ga]/[In+Ga]=0.55 ±0.05. For Cu-excess

grown films, KCN (aq.) etching to remove $Cu_x(SeS)_y$ was performed before analyses, while as-grown films were used for the analyses of Cu-poor grown films.

Figure 1 shows the relation between the concentration ratios of Y≡[S]/[Se+S] in the flux and in the film. The distinct change in Y_{film} from Cu-poor grown (open symbol) to Cu-excess grown (close symbol) films has previously been reported[1,2]. The solid lines are drawn by fitting the data to:

$$[S]_{film}/[Se]_{film} = C\cdot[S]_{flux}/[Se]_{flux} \quad (1)$$

or

$$Y_{film}/(1-Y_{film}) = C\ Y_{flux}/(1-Y_{flux})$$

where C is a constant for given temperature, which is based on a reaction model proposed for Ga(AsP)[3]. For Cu-poor grown films, the behavior of the preferred chalcogen incorporation is fit well by Eq. 1. reaction model. At T_{SS} = 450°C (△) or 550 °C (○), all data are on the line with C=0.32. At T_{SS} = 300°C (□), C=0.67 is found. On the other hand, for films grown with [Cu]/[In+Ga] > 1, the departure from the line with C = 4.2 is shown for the films grown at 300°C (■) with Y_{flux} > 0.3 although the others are on that line. This suggests that a difference in the reaction process determining the incorporation reaction of chalcogen between at 300°C and at higher temperatures.

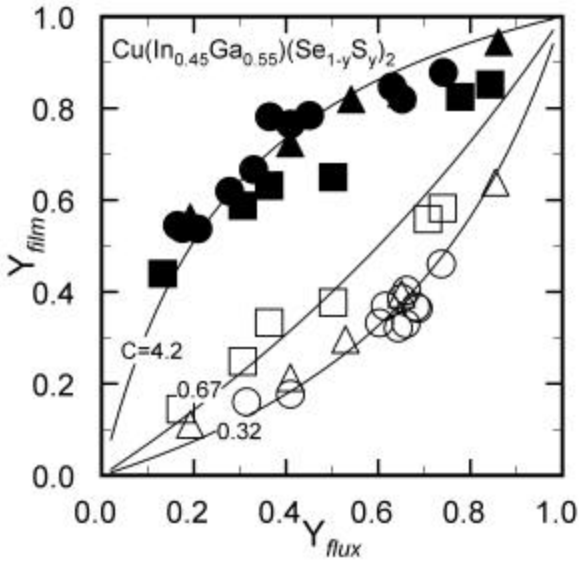

Figure 1. Relation between the [S]/[S+Se] ratios of the film composition (Y_{film}) and flux rate (Y_{flux}). The shape of symbol corresponds to the substrate temperature grown. Temperature: (■,□) 300°C, (▲,△) 450°C, (●,○) 550°. Open and closed symbols correspond to the Cu-poor and Cu-excess deposition condition, respectively.

Recent status of Cu(InGa)(SeS)$_2$ solar cell

In Table I, the recent status of Cu(InGa)$(SeS)_2$ (CIGSS) solar cells is listed. All samples were prepared by uniform deposition at about 550°C of substrate temperature. In Table I, not only the

solar cell performances of samples with $E_g > 1.5$ eV but also those with $E_g < 1.5$ eV are shown. For those with ~1.5 eV, good reproducibility of an efficiency of over 11% is demonstrated.

Table I. Recent results on solar cell performances using evaporated $Cu(InGa)(SeS)_2$ (w/o A.R. coat)

Cell	Eff. (%)	V_{OC} (V)	J_{SC} (mA/cm^2)	FF (%)	E_g (eV)
24428.22.6	11.0	0.848	17.8	0.732	1.57
24429.12.4	10.3	0.851	17.7	0.683	1.60
24430.12.6	11.1	0.844	18.2	0.722	1.58
24433.12.4	11.9	0.827	19.8	0.727	1.51
24434.22.4	11.4	0.849	19.3	0.695	1.53
24439.22.5	12.7	0.818	21.6	0.719	1.44
24440.32.4	14.5	0.776	24.3	0.767	1.37
24442.22.1	14.9	0.725	26.1	0.787	1.32

$Cu(InGa)(SeS)_2$ Formation by H_2Se/H_2S Reaction

The formation of $Cu(InGa)(SeS)_2$ absorber layers by the 2-step H_2Se/H_2S reaction of Cu-In-Ga precursor films has been previously demonstrated to yield homogenous Ga distribution and high device efficiency.[4,5] Recent work at IEC has indicated that the preferential reaction of Se with In and S with Ga plays a significant role in the 2-step reaction process. At the end of the selenization (first) step, the film is primarily composed of $CuInSe_2$ and a Cu_9Ga_4 intermetallic, which then reacts with S and incorporates into the chalcopyrite phase during the second step. Typically the selenization is carried out at 450ºC, while the sulfization is carried out at 550ºC.

The mechanism of Ga incorporation into the chalcopyrite phase during the sulfization reaction is not well understood, however. To gain further insight into the Ga incorporation into the chalcopyrite, films were reacted by the 2-step H_2Se/H_2S process, with the selenization carried out at 450ºC for 15 minutes and the sulfization carried out for 30 minutes at temperatures ranging from 450ºC to 550ºC. Films were characterized by EDS and XRD to measure the degree of Ga homogenization within the films.

The results show an increase in the measured [Ga]/[In+Ga] ratio with increasing temperature, as shown in Figure 2. The XRD results, shown in Figure 3, however, indicate a discontinuity at approximately 500ºC of the d-spacing determined from the maximum intensity of the chalcopyrite (112) peak. It should be noted that the d-spacings presented in the figure are somewhat oversimplified, as a number of the XRD patterns, especially those of samples sulfized at temperatures below 500ºC, had broadened peaks indicating some degree of composition grading. Further analysis is underway. A possible cause for a transition is suggested by the Cu-Ga phase diagram. At 485ºC the high-Ga boundary of the $\gamma 1$ (Cu_9Ga_4) phase transitions from a solid-solid boundary with the $\gamma 2$ phase to a solidus with a Ga-rich liquid phase.

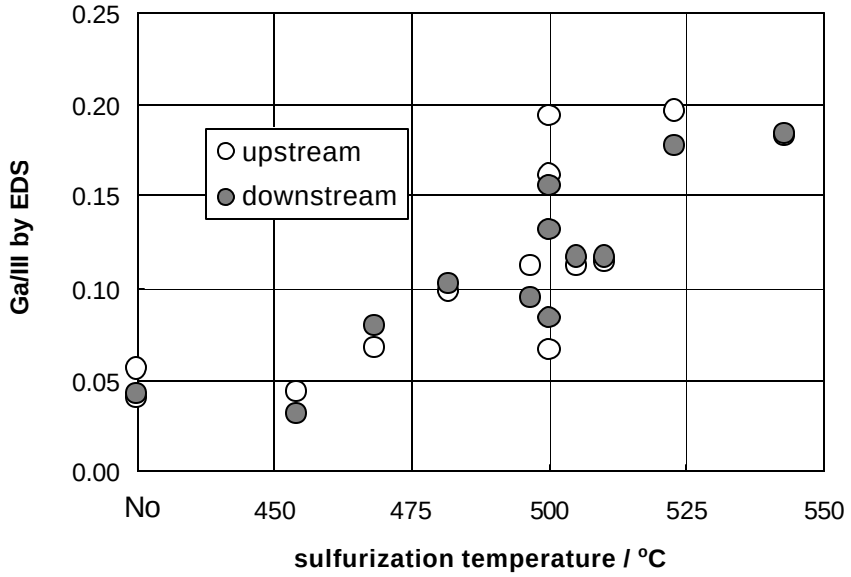

Figure 2. Ga/III ratio measured by EDS at the Cu(InGa)$(SeS)_2$. "No" indicates selenization only. "upstream" and "downstream" indicate sample position for a given run.

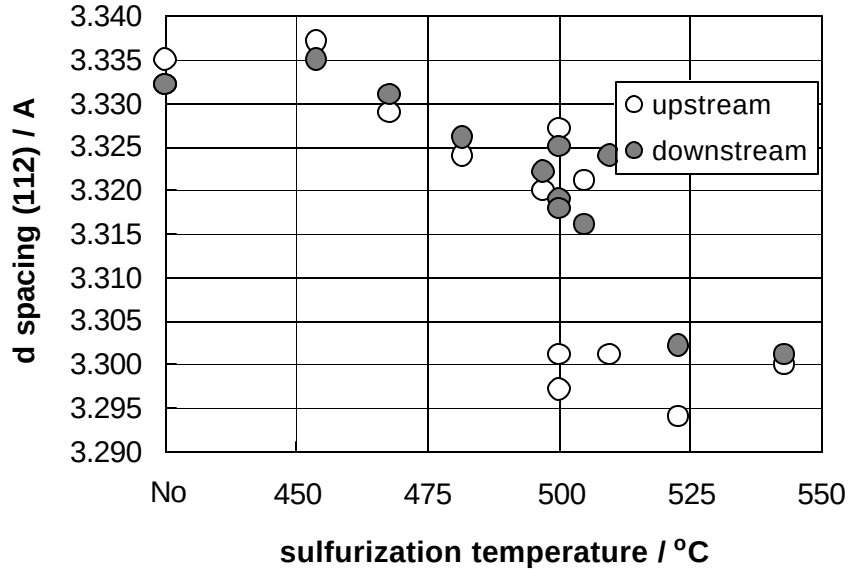

Figure 3. Highest-intensity (112) d-spacing measured by CuKa_1 q-2q XRD.

Improved Performance with Absorber Thickness < 1 µm

The effect of thickness (d) on morphology has been characterized for Cu(InGa)Se_2 films evaporated for different times using a single-layer uniform flux process. Parameters for 6 runs

with different times are listed in Table II. This includes the thickness measured by the mass increase of the substrate which is decreases linearly with deposition time. Evaporation source temperatures were the same for all the runs so they should have the same compositions. The compositions measured by EDS show a decrease in [Cu]/[In+Ga] but this may be an artifact of the measurement as the d becomes less than the penetration depth of the electrons.

AFM images with decreasing thickness are shown in Figure 4 for four of the films. This shows a change in morphology and decrease in grain size and the grain size with submicron thicknesses is significantly reduced. Further characterization is underway to determine if there is a coalescence of the grains as the thickness increases.

Table II. $Cu(InGa)Se_2$ films deposited for different times and rms roughness determined form AFM measurements.

Run #	Dep. time (min)	d (μm)	[Cu]/[In+Ga]	[Ga]/[In+Ga]	R_{ms} (nm)
34144	90	3.5	0.97	0.29	38
34143	60	2.2	0.95	0.32	45
34145	30	1.1	0.90	0.31	29
34148	20	0.76	0.89	0.31	28
34153	15	0.50	0.92	0.31	29
34149	10	0.35	0.85	0.31	16

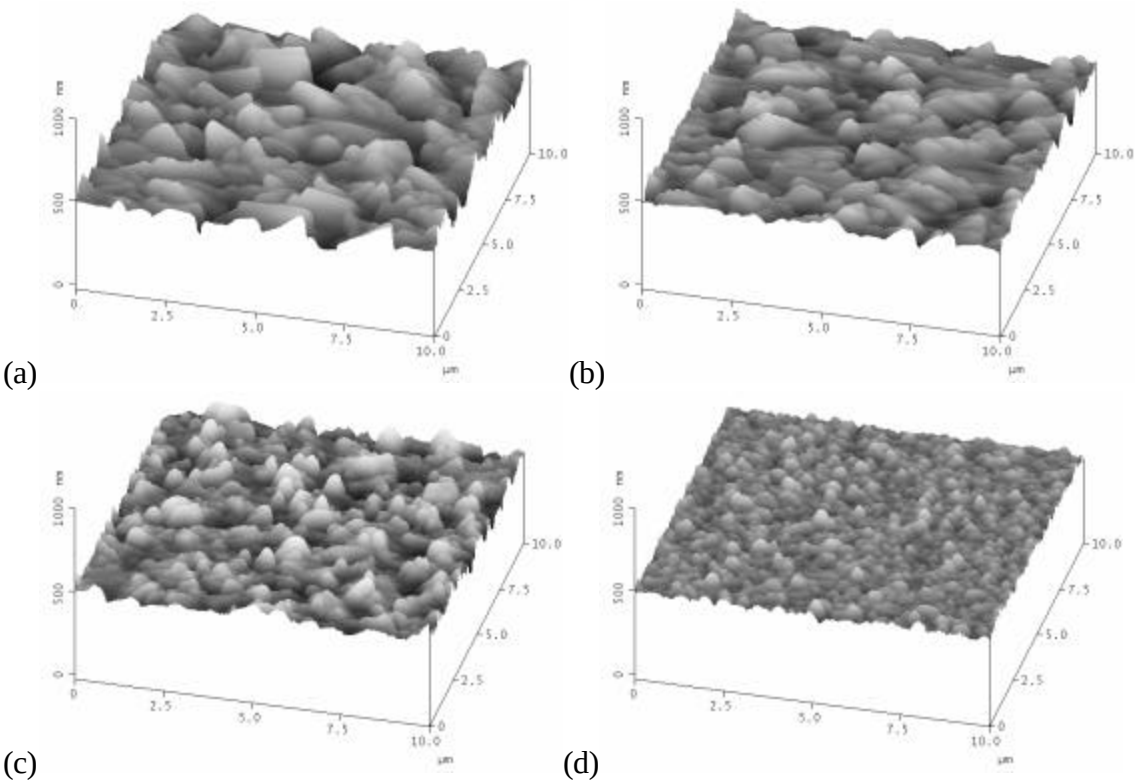

Figure 4. AFM images of films with thickness (a) 2.2 µm, (b) 1.1 µm, (c) 0.5 µm, and (d) 0.35 µm. Each image shows a 10 x 10 µm area.

Best regards,

Robert W. Birkmire
Director

CC: Paula Newton, IEC
Susan Tompkins, RGS
Carolyn Lopez, NREL

References

1 A. Stavrides, C. Yapp, W. N. Shafarman, R. Aparicio, R. Opila, and R. W. Birkmire, Proc. 31st IEEE PVSC, 247 (2005).
2 R. Klenk, T. Walter, D. Schmid, and H. W. Schock, Jpn. J. Appl. Phys. Suppl. **32**, 57 (1993).
3 B. W. Liang and C. W. Tu, J. Appl. Phys. 74, 255 (1993).
4 V. Alberts, J. Titus, and R. W. Birkmire, Thin Solid Films **451-452**, 207 (2004).
5 G.M. Hanket, W.N. Shafarman, and R.W. Birkmire, Proc. 4th WCPEC, 560 (2006).